MEaSUREs Greenland Ice Velocity: Selected Glacier Site Velocity Maps from Optical Images, Version 3

USER GUIDE

How to Cite These Data

As a condition of using these data, you must include a citation:

Howat, I. 2021. *MEaSUREs Greenland Ice Velocity: Selected Glacier Site Velocity Maps from Optical Images, Version 3*. [Indicate subset used]. Boulder, Colorado USA. NASA National Snow and Ice Data Center Distributed Active Archive Center. https://doi.org/10.5067/RRFY5IW94X5W. [Date Accessed].

FOR QUESTIONS ABOUT THESE DATA, CONTACT NSIDC@NSIDC.ORG

FOR CURRENT INFORMATION, VISIT https://nsidc.org/data/NSIDC-0646

NSIDC National Snow and Ice Data Center

TABLE OF CONTENTS

1 DATA DESCRIPTION

1.1 Parameters

This data set reports the following parameters:

- Ice velocities (x- and y- components)
- Error estimates (x- and y-components)
- Magnitude of ice velocities (available for data from 2016 to the present, only)

All parameters are in meters per year.

The NoData value for this data set is -99999.

Corresponding ASCII text metadata files (`.meta`) are also provided and contain geographical information plus dates and codes that reveal the sensor combinations of the images used to create the monthly mean. The sensor combination key is provided in Table 1.

Table 1. Sensor Key for Metadata Files

Sensor	Code
Landsat 8 OLI	LC08
Landsat 7 ETM+	LE07
Landsat 5 TM	LT05
Landsat 4 TM	LT04
ASTER	ASTR

The following sensor combinations are possible: LT04/LT04, LT04/LT05, LT05/LT05, LT05/LE07, LT05/ASTR, LE07/LE07, LC08/LC08, LE07/LC08, ASTR/ASTR, LE07/ASTR, LC08/ASTR.

1.2 File Information

1.2.1 Format

This data set is organized into 74 study sites. Study sites in this data set correspond to geographical sub-regions of Greenland. The name of each sub-region reflects its center latitude. A table with the name (center latitude) of each sub-region, the latitude and longitude of its lower left corner, and the geographical features it contains is provided in the Appendix A of this User Guide.

1.2.2 File Contents

The following files are provided for each site:

- Velocity browse image (PNG)
- Component velocity in the x-direction (GeoTIFF)
- Component velocity in the y-direction (GeoTIFF)
- Velocity magnitude (GeoTIFF; available for files from 2016 to the present, only)
- Error estimates in the x-direction (GeoTIFF)
- Error estimates in the y-direction (GeoTIFF)
- Metadata file (ASCII text)

There is also a shapefile, which includes the locations of all the grids used (see Section 1.3.1 for more details). The shapefile (nsidc0646_spatial_coverage_v03.0.shp) and the associated files can be found in the earliest dated folder 1985.03.01 on HTTPS, or in Earthdata Search (by sorting the file list by start date, earliest first). Click here to access the shapefile.

1.2.3 Naming Convention

This section describes the naming convention for this product. Refer to Table 2 for descriptions of each variable of the file naming convention.

File Naming Convention:

`OPT_[sub-region]_[date]_[datum]_[v0N.n].[ext]`

Example File Names:

- `OPT_E61.10N_2019-12_vv_v03.0_preview.png`
- `OPT_E61.10N_2019-12_vx_v03.0.tif`
- `OPT_E61.10N_2019-12_vy_v03.0.tif`
- `OPT_E61.10N_2019-12_vv_v03.0.tif`
- `OPT_E61.10N_2019-12_ex_v03.0.tif`
- `OPT_E61.10N_2019-12_ey_v03.0.tif`
- `OPT_E61.10N_2019-12_v03.0.meta`

Table 2. File Name Variables and Descriptions

Variable	Description
`OPT`	Velocities derived from optical image pairs acquired by Landsat 8 OLI, Landsat 7 ETM+, Landsat 4 TM, Landsat 5 TM, ASTER or a combination.
`sub-region`	Sub-region names are defined as follows: • E, W, N, or S: East, West, North, or South Coast • Center latitude in decimal degrees
`date`	Date of acquisition (YYYY-MM)

Variable	Description
`datum`	Component velocity or component error estimate: • vx: x-component of velocity • vy: y-component of velocity • vv: magnitude of velocity • ex: x-component of error • ey: y-component of error
`v0N.n`	Version number
`.ext`	File extension: • `_preveiw.png`: Portable Network Graphic file • `.tif`: GeoTIFF-formatted file • `.meta`: ASCII text file. Contains image dates, production date, sensor combinations, and geographical information.

1.3 Spatial Information

1.3.1 Coverage

This data set contains velocity maps for most of the outlet glaciers on the Greenland Ice Sheet. Figure 1**Error! Reference source not found.** shows the locations of all grids on a map of Greenland. The study area lies within the following bounding box:

- Southernmost Latitude: 60° N
- Northernmost Latitude: 82° N
- Easternmost Longitude: 20° W
- Westernmost Longitude: 70° W

1.3.2 Resolution

100 meters

1.3.3 Projection and Grid Description

GeoTIFFs are provided in a WGS 84 polar stereographic grid with a standard latitude of 70° N and rotation angle of -45° (sometimes specified as a longitude of 45° W). With this convention, the y-axis extends south from the North Pole along the 45° W meridian (EPSG:3413).

Table 3. Northern Hemisphere Projection Based on WGS 1984 (EPSG: 3413)

Geographic coordinate system	WGS 84
Projected coordinate system	World Geodetic System 1984
Longitude of true origin	-45

Latitude of true origin	70
Scale factor at longitude of true origin	1
Datum	WGS 84
Ellipsoid/spheroid	WGS 84
Units	Meter
False easting	0
False northing	0
EPSG code	3413
PROJ4 string	proj4.defs("EPSG:3413","+proj=stere +lat_0=90 +lat_ts=70 +lon_0=-45 +k=1 +x_0=0 +y_0=0 +datum=WGS84 +units=m +no_defs");
Reference	https://epsg.io/3413

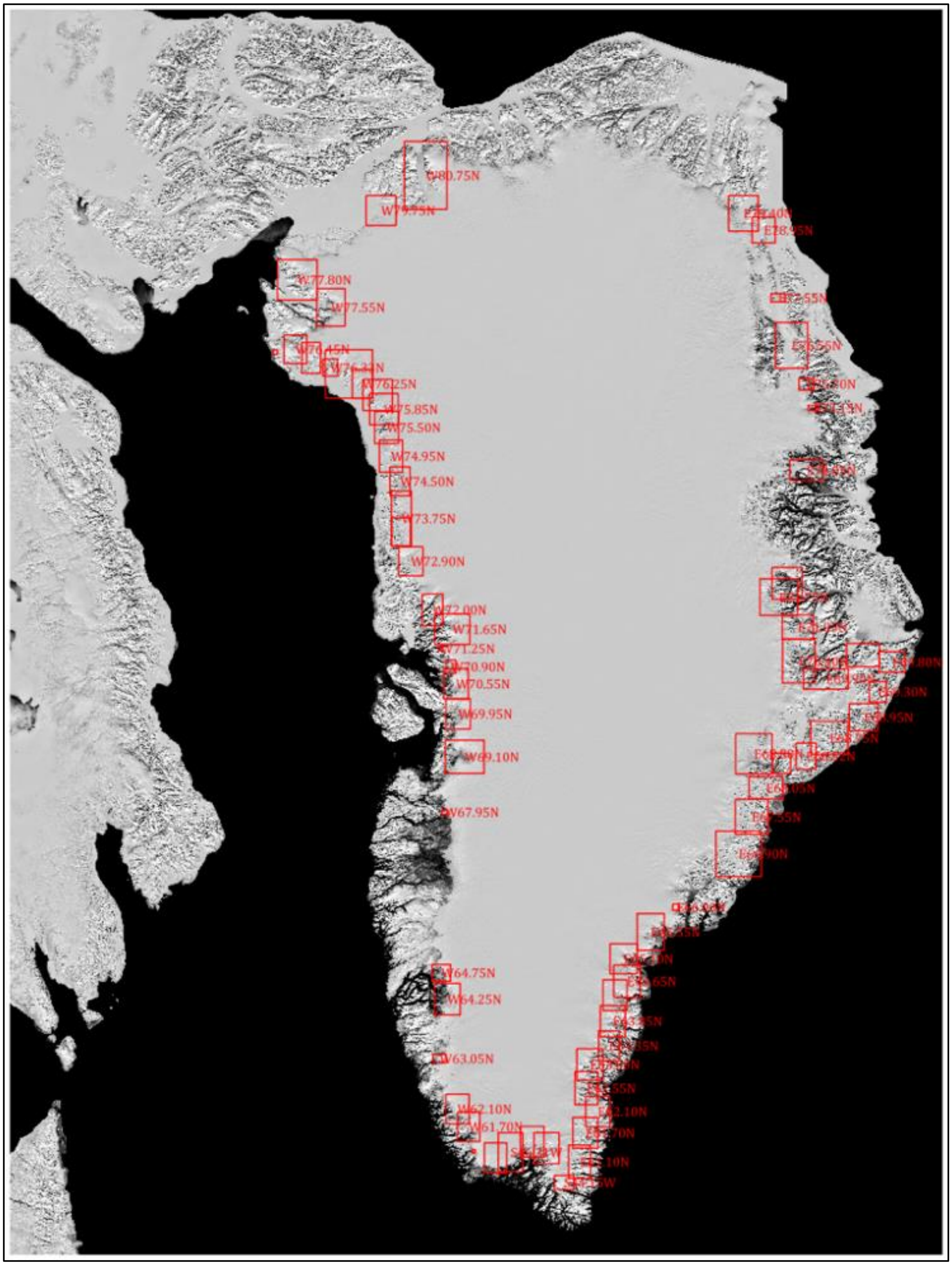

Figure 1. Gridded Spatial Coverage Map. See Appendix B to download a high-resolution version of this image.

1.4 Temporal Information

1.4.1 Coverage

01 March 1985 to 31 December 2020

1.4.2 Resolution

Monthly

2 DATA ACQUISITION AND PROCESSING

2.1 Acquisition

All Level-1 Landsat imagery was obtained from the U. S. Geological Survey (USGS | Landsat Level 1 Standard Data Products). ASTER (AST14DMO) imagery was obtained from the NASA Land Processes Distributed Active Archive Center (LP DAAC).

2.2 Processing

These data were created using orthorectified Landsat Level L1T or L1G and ASTER (AST14DMO) imagery. Orthorectified images were received in UTM projection and converted to Polar Stereographic using Geographic Data Abstraction Library (GDAL) software. ASTER visible bands 1-3 were reduced to a single grayscale principal component image. The panchromatic band was used for Landsat 7 and 8. For Landsat 4 and 5 TM images, bands 2, 3, and 4 were reduced to a single grayscale principal component image. Velocity fields were constructed using images from the same sensor or combinations of Landsat 4, Landsat 5, Landsat 7, Landsat 8, and ASTER images. In most cases, only Landsat images from the same path/row were correlated to reduce the impact of terrain-dependent errors.

Velocity fields were produced by an automated cross-correlation of sequential images using the Multi-Image Multi-Chip (MIMC) algorithm described in Ahn and Howat (2011) and updated in Jeong et al. (2017). The MIMC utilizes a range of image filters and search window sizes as well as both backward and forward matching to generate 64 matches per sample. Neighborhood statistics and an *a priori* velocity field, consisting of radar-derived velocities closest in time to the image dates from the *MEaSUREs Greenland Ice Sheet Velocity Map from InSAR Data* data set, were used to select the highest confidence solution and its uncertainty.

This velocity field was then corrected for image re-registration errors by subtracting the average displacement over bedrock or very slow-moving ice (< 10 m/year), which is located using the *a* *priori* velocity field. The residual deviation of velocities over bedrock then provides the registration error (see the Error Sources section). Individual velocity image pairs within each region were sampled to the same grid and stacked into monthly medians at each grid point, providing a monthly sampling. The median error was also obtained.

In Version 3, data from 01 January 2016 onwards were revised using only Landsat 8 OLI imagery as input. The MIMC algorithm was replaced with the feature tracking algorithm within the Surface Extraction through TIN Searchspace Minimization (SETSM) open-source photogrammetry software package (described in Noh and Howat, 2019 and on Github). Whereas MIMC was specifically designed for lower bit resolution images (ASTER and Landsat 7 or earlier) and challenges arising from the SLC-off Landsat 7 EMT+ imagery, SETSM provides more efficient processing of Landsat 8 OLI imagery in high-performance computing environments. This allows the processing of image pairs at a higher spatial resolution. The same basic procedure, cross-correlation based pixel matching, is common to both algorithms. The processing steps remain the same except that this version uses distance-weighted averaging between overlapping processing regions when building monthly mosaics, whereas previous versions did not.

Note: Monthly means are calculated from images, which may have acquisition dates from the preceding or succeeding month. For the naming convention, the month is determined from where the midpoint Julian dates fall. For example, September monthly means may have been generated from images that were acquired in August or in October but the midpoint Julian date between the images falls within September. The exact dates used are included in the `.meta` file.

2.3 Quality, Errors, and Limitations

Uncertainty in the velocity solution results from uncertainty in the match solution and uncertainty in image co-registration. Match solution uncertainty is estimated at each grid point from the sample of individual velocity solutions that results from the MIMC procedure. This error is typically on the order of one-third of a pixel. Co-registration error, the dominant source of uncertainty, is estimated from the residual velocities obtained over bedrock and very slow ice after the mean is removed. These errors vary considerably, but are typically on the order of 100 m/year.

In Version 3 (for data post-2016), error estimates are obtained from the standard deviation of speed measurements on ice-free surfaces, which are then combined as median values at each pixel for each pair solution when constructing monthly estimates. Additionally, in this version, displacements of icebergs and floating ice mélange are not masked as in previous versions and may cause very large values near the ice front. These can be masked using the GIMP ice mask products (e.g., the *MEaSUREs Greenland Ice Mapping Project Land Ice and Ocean Classification Mask*).

2.4 Instrument Description

The Advanced Spaceborne Thermal Emission and Reflection Radiometer (ASTER) obtains high-resolution (15 to 90 square meters per pixel) images of the Earth in 14 different wavelengths of the electromagnetic spectrum, ranging from visible to thermal infrared light. ASTER was launched in December 1999 onboard Terra, the flagship satellite of NASA's Earth Observing System (EOS). For more information, see NASA's Terra | ASTER web page.

The Enhanced Thematic Mapper Plus (ETM+) instrument on board Landsat 7 is a fixed "whisk-broom," eight-band, multispectral scanning radiometer capable of providing high-resolution imaging information of the Earth's surface. Orbiting at an altitude of 705 km, the instrument detects spectrally-filtered radiation in visible near-infrared, short-wave near-infrared, long-wave near-infrared, and panchromatic bands from the sun-lit Earth in a 183 km wide swath. Onboard Landsat 4 and Landsat 5, the Thematic Mapper (TM) image data files consist of seven spectral bands. The resolution is 30 m for bands 1 to 7. Thermal infrared band 6 was collected at 120 m, but was resampled to 30 m. The approximate scene size is 170 km north-south by 183 km east-west (106 mi by 114 mi). For more information, visit NASA's Landsat Science | The Enhanced Thematic Mapper Plus web page.

The Operational Land Imager (OLI) on Landsat 8 is an enhanced version of Landsat 7's ETM+ that adds two new spectral bands: a deep blue visible channel (Band 1), specifically designed for water resources and coastal zone investigation; and a new infrared channel (Band 9) to detect cirrus clouds. For more information, visit the USGS Landsat 8 web page.

3 SOFTWARE AND TOOLS

GeoTIFF files can be viewed with a variety of Geographical Information System (GIS) software packages including:

- Blue Marble Geographics Global Mapper
- QGIS
- GDAL
- Esri ArcGIS

4 VERSION HISTORY

Table 4. Version History Summary

Version	Release Date	Description of Changes
V1	March 2016	Initial release

Version	Release Date	Description of Changes
V2	May 2017	Changes for Version 2 include: A correction was applied in the processing, which caused error values to appear as NaNs in some of the data A more aggressive filtering method was applied to remove small, isolated clusters of data Cross-path Landsat pairs were used to fill in temporal gaps in the 2016 data, using the MEaSUREs Greenland Ice Mapping Project (GIMP) Digital Elevation Model from GeoEye and WorldView Imagery data set and the orthorectification algorithm of Rosenau (2012). Spatial coverage was expanded to include the W80.75N grid Temporal coverage was expanded from September 2015 to September 2016 To reduce overall size of the data set, GeoTIFFs are produced using Lempel–Ziv–Welch LZW lossless compression
V2 (update)	October 2017	Temporal coverage expanded to 1985-2016 using data from Landsat 4 and 5 A more aggressive filtering method was applied to remove the following small, isolated clusters of data: Ecoast-62.10N: OPT_E62.10N_2003-09, OPT_E62.10N_2003-10, OPT_E62.10N_2004-09, OPT_E62.10N_2004-10 Ecoast-64.65N: OPT_E64.65N_2011-09, OPT_E64.65N_2011-10 Spatial coverage was increased by 24 new grids
V2.1	July 2019	This minor version provides all available data from 1985 through 2018 for all regions. Additionally, the sensor name abbreviations in the .meta files have changed. The new abbreviations are listed in Table 1.

Version	Release Date	Description of Changes
V3	September 2020	Changes in Version 3 apply only to data from 01 January 2016 to 31 December 2019; data files prior to 2016 are identical to Version 2.1. This update utilizes a new feature tracking algorithm within the Surface Extraction through TIN Searchspace Minimization (SETSM) software package, adopted because it is open source and optimized for high-performance computing environments. This update only uses Landsat 8 OLI imagery For data from 01 January 2016 onwards, there is one additional geoTIFF available for velocity magnitude, (vv). Some data files that were available in previous versions did not meet the new algorithm's requirements and were removed. See Appendix B for a list of removed files. When the data set was originally released on 16 September 2020, it inadvertently contained Version 2 data files for the period 01 January 2016 – 31 December 2018. These files were replaced with the correct versions on 12 October 2020.
V3	August 2021	This update includes the following: Temporal coverage extended to 31 December 2020

5 RELATED DATA SETS

Greenland Ice Sheet Mapping Project (GIMP)

6 RELATED WEBSITES

MEaSUREs at NSIDC | Overview

7 CONTACTS AND ACKNOWLEDGMENTS

Ian Howat
Ohio State University
Byrd Polar Research Center

Acknowledgments:

These data were generated through a grant from the NASA MEaSUREs program.

8 REFERENCES

Yushin Ahn, & Howat, I. M. (2011). Efficient Automated Glacier Surface Velocity Measurement From Repeat Images Using Multi-Image/Multichip and Null Exclusion Feature Tracking. *IEEE*

Transactions on Geoscience and Remote Sensing, 49(8), 2838–2846. https://doi.org/10.1109/tgrs.2011.2114891

Enderlin, E. M., Howat, I. M., Jeong, S., Noh, M.-J., van Angelen, J. H., & van den Broeke, M. R. (2014). An improved mass budget for the Greenland ice sheet. *Geophysical Research Letters*, 41(3), 866–872. https://doi.org/10.1002/2013gl059010

Howat, I. M., Ahn, Y., Joughin, I., van den Broeke, M. R., Lenaerts, J. T. M., & Smith, B. (2011). Mass balance of Greenland's three largest outlet glaciers, 2000-2010*. Geophysical Research Letters*, 38(12). https://doi.org/10.1029/2011gl047565

Jeong, S., & Howat, I. M. (2015). Performance of Landsat 8 Operational Land Imager for mapping ice sheet velocity. *Remote Sensing of Environment*, 170, 90–101. https://doi.org/10.1016/j.rse.2015.08.023

Jeong, S., Howat, I. M., & Ahn, Y. (2017). Improved Multiple Matching Method for Observing Glacier Motion with Repeat Image Feature Tracking. *IEEE Transactions on Geoscience and Remote Sensing*, 55(4), 2431–2441. https://doi.org/10.1109/tgrs.2016.2643699

Noh, M.J., & Howat, I. M. (2019). Applications of high-resolution, cross-track, pushbroom satellite images with the SETSM algorithm. *IEEE Journal of Selected Topics in Applied Earth Observations and Remote Sensing*, 12(10), 3885–3899. https://doi.org/10.1109/JSTARS.2019.2938146

Rosenau, R., Dietrich, R., & Baessler, M. (2012). Temporal flow variations of major outlet glaciers in Greenland using Landsat data. In 2012 *IEEE International Geoscience and Remote Sensing Symposium*. IEEE. https://doi.org/10.1109/igarss.2012.6351100

9 DOCUMENT INFORMATION

9.1 Publication Date

September 2020

9.2 Date Last Updated

06 August 2021

APPENDIX A – Grid Names, Locations, and Features

Table A1. Grid Names, Locations, and Geographical Features

Grid Name lat, lon of lower left corner	Geographical Features in Grid
E61.10N 60.8004, -43.9589	Unnamed glacier near Danell Fjord Danells Kanderdluluk Fjord Cape Herluf Trolle Cape Tordenskjold
E61.70N 61.3903, -43.7671	Anorituup Kangerlua Fjord Napasorsuaq Fjord
E62.10N 61.801, -43.2149	Puisortoq Glacier (north) Puisortoq Fjord (south)
E62.55N 62.2422, -43.6371	Mogens Heinesen Fjord Timmiarmiut Fjord
E63.00N 62.7212, -43.5332	Heimdal Glacier
E63.35N 63.0911, -42.5656	Thrym Glacier Sehested Fjord Skinfaxe Glacier
E63.85N 63.5620, -42.4419	Bernstorffs Fjord
E64.35N 64.0768, -42.2688	Gyldenlove Fjord
E64.65N 64.3291, -41.7539	Fridtjof Nansens Peninsula
E65.10N 64.7987, -41.8569	Koge Bay
E65.55N 65.2242, -40.5156	Ikertivaq Sound Pamiatig
E66.00N 65.9492, -38.6334	Bruckner Heim
E66.50N 66.1973, -39.1116	Fenris Glacier Helheim Glacier
E66.60N 66.3305, -37.4428	Midgard Glacier Midgard North

Grid Name **lat, lon of lower left corner**	**Geographical Features in Grid**
E66.90N 66.5045, -36.2923	Kruuse Fjord Steenstrup Glacier Tasiilaq Fjord
E67.55N 67.2762, -34.9643	Norde Parallel Glacier Nordre
E68.05N 67.9148, -33.9170	Hutchinson Glacier
E68.50N 68.3044, -31.1040	Courtauld Glacier Frederiksborg Glacier Christian IV Glacier Sorgenfri Glacier
E68.52N 68.3044, -31.1040	Schjelderup Glacier Sorgenfri Glacier
E68.75N 68.5151, -30.1133	Rosenborg Kronborg Borggraven
E68.80N 68.4663, -34.3672	Kangerdlussuaq Glacier Nordfjord Glacier
E68.95N 68.7516, -27.7071	Sortebrae
E69.30N 69.1760, -26.1549	Barclay Bay unnamed glacier
E69.80N 69.6752, -25.0537	Steno Bartholin
E69.90N 69.8224, -29.5537	unnamed glaciers
E70.10N 70.0023, -26.7390	Syd Glacier
E70.40N 70.0488, -30.6613	Rolige Glacier
E71.05N 70.9090, -30.0003	Harefjord Rypefjord unnamed glacier
E71.75N 71.4887, -30.9758	Daugaard-Jensen Glacier
E71.95N 71.7410, -29.9742	Daugard-Jensen Glacier

Grid Name **lat, lon of lower left corner**	**Geographical Features in Grid**
E74.05N 73.9482, -26.4408	Waltershausen
E75.15N 75.1665, -23.2614	Heinkel
E75.70N 75.6225, -23.3212	Ejnar Mikkelsen Storm Stejl
E76.55N 76.2080, -24.5210	Bistrup Brede Storstrommen
E77.55N 77.51625, -22.7208	Kofoed-Hansen
E78.95N 78.7851, -22.2120	Gammel Hellerup Glacier
E79.40N 79.190, -24.0779	Fjorden
W61.30N 61.2671, -47.8697	unnamed
W61.70N 61.4746, -48.4912	Sermiligarssuk Fjord
W62.10N 61.8077, -49.0172	Nigerdlikasik Glacier Avangnardleq Glacier Ukassorssuaq
W63.05N 62.9804, -49.7627	Nakaissorssuaq
W64.25N 63.9263, -49.8721	Kangiata Nunata Sermia Glacier Quamanarssup Glacier
W64.75N 64.4610, -50.1732	Ujarassuit Paauat Fjord Narsap Sermia Glacier
W67.95N 67.9133, -50.3921	Usulluup
W69.10N 68.7418, -50.4126	Alangordliup Sermia Glacier Jakobshavn Isbræ Glacier Torsukattak Glacier
W69.95N 69.6356, -50.6122	Kangilerngata Sermia Glacier Kujatdleq Glacier Torsukattak Fjord

Grid Name **lat, lon of lower left corner**	**Geographical Features in Grid**
W70.55N 70.2285, -50.9177	Lille Glacier Sermilik Glacier Kangilleq Glacier Store Glacier
W70.90N 70.7542, -50.9613	Perdlerfiup Sermis Glacier Silardleq
W71.25N 71.1917, -51.5587	Kangerdluarssup
W71.65N 71.3100, -51.8327	Kangerluarsuk Glacier Rink Glacier
W72.00N 71.6540, -52.8014	Inngia Fjord Umiammakku Glacier
W72.90N 72.5829, -54.8293	Alangorssup Sermia Glacier Upernavik Isstorm Glacier
W73.45N 73.1520, -55.6912	Kakivfait Sermiat Glacier Giesecke Glacier Nutarmiut Glacier Tuvssaq (populated area)
W73.75N 73.1520, -55.6912	Cornell Glacier Sugarloaf Bugt (sound) Ussing Glacier
W74.50N 74.1506, -56.4843	Cornel Glacier Alison Bugy (bay) Illulik (populated area)
W74.95N 74.5750, -57.6463	Hays Glacier Kjer Glacier Jensen Glacier
W75.50N 75.1264, -58.5281	Dietrichson Glacier Steenstrup Glacier Sverdrup Glacier
W75.85N 75.4736, -59.2722	Nansen Glacier Nordenskiold Glacier
W76.10N 75.7205, -60.0987	Kong Oscar Glacier Nordenskiold Glacier Nutarmiut

Grid Name **lat, lon of lower left corner**	**Geographical Features in Grid**
W76.25N 75.9067, -61.2365	Balgoni Docker Smith Glacier Fisher Igssuarssuit Sermia Glacier Leven
W76.30N 76.1846, -68.8535	Pituffik
W76.33N 76.1538, -64.2165	Yngvar Nielsen Glacier Mohn Glacier
W76.35N 75.7416, -63.3988	Mohn Glacier Gade Glacier Meteor Bay Yngvar Nielson Glacier
W76.40N 76.0579, -65.9643	Savigssuaq Helland Sidebriks
W76.45N 76.1084, -67.6907	Dedodes Harald Moltke
W77.55N 77.0728, -66.2296	Leidy Mane Heilprin Mellville Tracy
W77.80N 77.2407, -70.5337	Qaqortaq Boudoin
W79.75N 79.3702, -65.1597	Humboldt
W80.75N 81.1505, -46.6109	Chow
S44.15W 60.5845, -44.5380	unnamed glacier
S44.84W 61.0923, -45.3465	Kiattuut Sermiat Glacier Qooroq Fjord
S45.43W 61.2196, -45.8994	Equlorutsit Kangigdlit Sermia
S46.31W 60.9223, -46.7905	Eqalorutsit Kangigdlit Sermia West

Grid Name **lat, lon of lower left corner**	**Geographical Features in Grid**
S46.91W 60.8876, -47.3303	Qaleragdlit Naujat Sermilik

APPENDIX B – HIGH RESOLUTION IMAGE

To download a high resolution of the Gridded Spatial Coverage Map, click here.

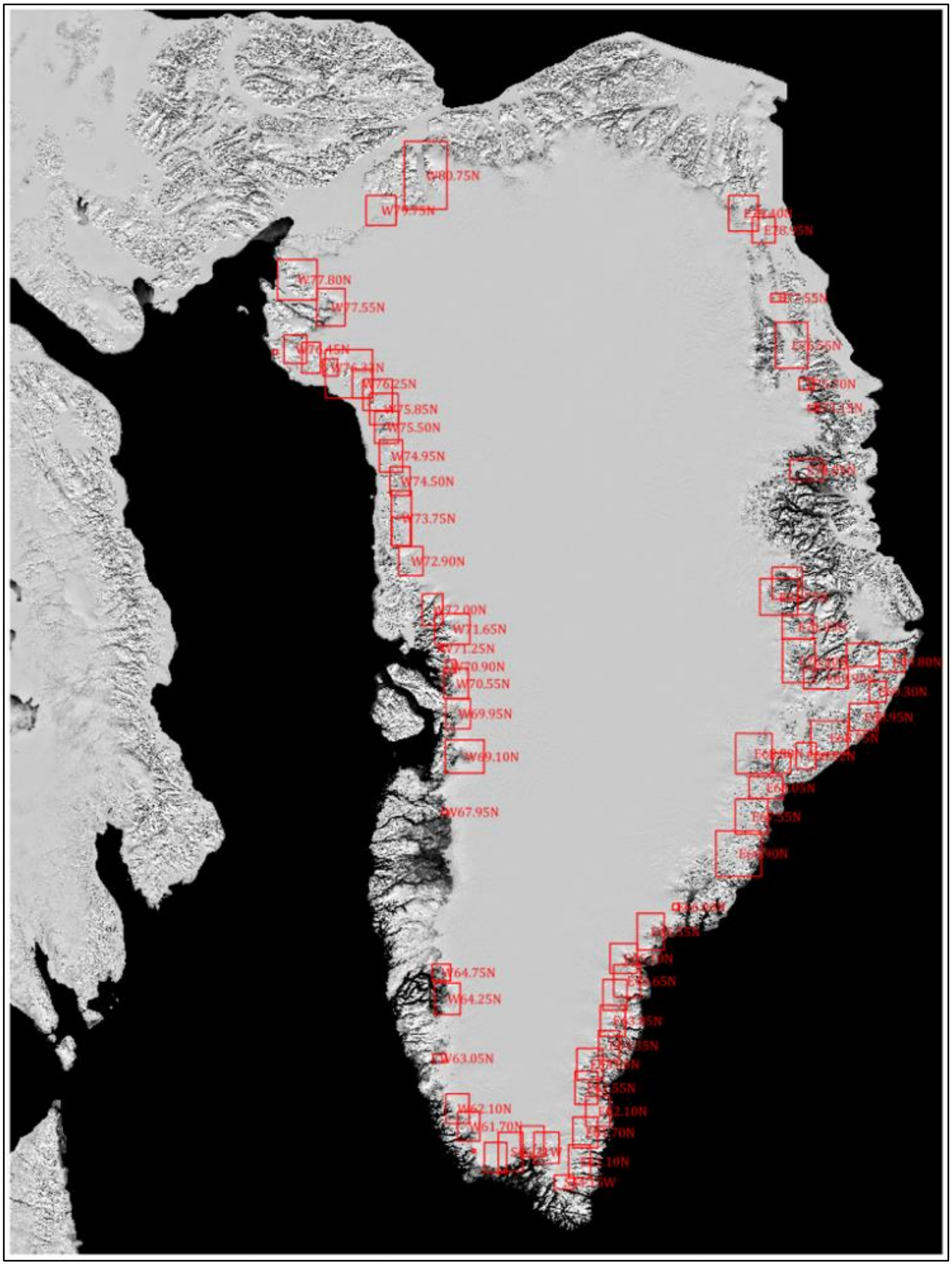

Figure 2. Gridded Spatial Coverage Map

APPENDIX C – Files Removed for Version 3

The following files were removed for Version 3:

OPT_E61.10N_2016-01
OPT_E64.65N_2018-02
OPT_E64.65N_2018-07
OPT_E65.55N_2018-10
OPT_E66.00N_2018-06
OPT_E66.90N_2018-11
OPT_E68.50N_2018-02
OPT_E75.15N_2018-03
OPT_E75.15N_2018-04
OPT_E75.15N_2018-05
OPT_E75.15N_2018-06
OPT_E75.15N_2018-07
OPT_E75.15N_2018-08
OPT_E75.15N_2018-09
OPT_E76.55N_2018-03
OPT_E76.55N_2018-04
OPT_E76.55N_2018-05
OPT_E76.55N_2018-06
OPT_E76.55N_2018-07
OPT_E76.55N_2018-08
OPT_E76.55N_2018-09
OPT_E76.55N_2018-10
OPT_E77.55N_2018-03
OPT_E77.55N_2018-04
OPT_E77.55N_2018-05
OPT_E77.55N_2018-06
OPT_E77.55N_2018-07
OPT_E77.55N_2018-08
OPT_E77.55N_2018-09
OPT_E77.55N_2018-10
OPT_E78.95N_2018-07
OPT_E78.95N_2018-08
OPT_E78.95N_2018-09
OPT_E79.40N_2018-06
OPT_E79.40N_2018-07
OPT_E79.40N_2018-08
OPT_E79.40N_2018-09
OPT_S44.15W_2016-01
OPT_S44.84W_2018-06
OPT_S45.43W_2016-01
OPT_S45.43W_2018-06
OPT_S45.43W_2018-09
OPT_S46.31W_2018-06
OPT_S46.31W_2018-09
OPT_W61.70N_2018-11
OPT_W61.70N_2018-12
OPT_W63.05N_2018-01
OPT_W63.05N_2018-06
OPT_W76.30N_2018-05
OPT_W76.30N_2018-07
OPT_W76.30N_2018-08
OPT_W76.30N_2018-10
OPT_W77.55N_2018-02